Digest Journal of Nanomaterials and Biostructures Vol. 18, No. 1, January - March 2023, p. 307 - 314

Investigation the effect of Co_3O_4 doping on structural and mechanical properties of ZnO pallets synthesized by powder metallurgy method a nd their biological evaluation

A. Shuaib[a,b,*], F. Mannan[a], Z. Ali[b], H. Rehman[c], M. H. Farooq[b], T. G. Shahzady[d]
[a]*Department of Physics, University of Engineering & Technology, Lahore 54890, Pakistan*
[b]*Department of Natural Sciences & Humanities, University of Engineering & Technology, New Campus, Lahore, Pakistan*
[c]*Department of Chemistry, University of Sahiwal, Sahiwal, Pakistan*
[d]*Department of Chemistry, Lahore Garrison University, Pakistan*

ZnO is an important semiconductor due to its unique structural, mechanical and optical properties. In this study pure ZnO pallets and Co_3O_4 doped ZnO pallets with varying molar concentration of dopant i.e 2% 4% 6% 8% and 10% were prepared by using hydraulic press. X-ray diffraction (XRD), FTIR and Vickers indentation method is used for pallets characterization. The XRD analysis revealed that the pure ZnO and doped ZnO pallet samples have hexagonal wurtzite structure. Vickers Hardness test showed that pure ZnO pallet has maximum hardness as compared to the Co_3O_4 doped ZnO pallets. FTIR analysis used to examine the bonding properties of synthesized Co doped ZnO. Doped materials with varying concentration were applied against different gram positive and gram negative bacterial strains. A considerable increase in antibacterial activity was observed by increasing the concentration of Co_3O_4 dopant.

(Received October 23, 2022; Accepted March 1, 2023)

Keywords: Co_3O_4 doped ZnO, Pallets, Vickers hardness

1. Introduction

In comparison to other metal oxides, Zinc oxide is a good candidate because of its optoelectronic uses in diodes, UV lasers, and gas sensors [1–3]. Now a day's ZnO semiconductors are being used in industries at very large scale. It is widely used in many industries such as paints, cosmetics, pharmaceuticals, plastic and rubber industry and in the formation of optoelectronic devices. At ambient temperature, Zinc oxide semiconductors at room temperature have a direct band gap of about 3.2 eV to 3.4 eV [4]. Oxygen vacancies and zinc interstitials are examples of intrinsic and extrinsic defects that have a significant impact on ZnO behavior. By releasing trapped electrons, oxygen vacancies, which are responsible for ZnO's n-type characteristic, result in increased electrical conductivity. Doping is the most important property of semiconductors by which we can change the electronic properties. Doping with materials is such property of semiconductors that increase the number of applications. Transition metal oxides show numerous properties due to their variable oxidation states. Co_3O_4 is a vital transition metal oxide because of its uses in various field of research and industry include pigments, gas sensor, magnetic materials, catalyst, electrochemical systems and high-temperature solar selective absorbers [5-10]. Doping of ZnO with transition metals, particularly cobalt has thus been extensively studied in order to modify its optical, magnetic, and photocatalytic properties [11, 12]. Recent research has shown that the optical, photocatalytic, and mechanical properties of Zno were significantly influenced by the position of dopant ions [13, 14]. ZnO nanoparticles have affinity for bacterial cells which is the important factor for antibacterial activity. It was mentioned by some researchers that ZnO nanoparticles could damage the membrane and kill the bacterial cells [15].

[*] Corresponding author: ahmadshuaib@uet.edu.pk
https://doi.org/10.15251/DJNB.2023.181.307

In this work structural and mechanical properties of ZnO doped with Co_3O_4 were investigated at different concentrations. The structural behavior was investigated by X-ray diffraction, FTIR analysis, while mechanical study was carried out by using Vickers Indentation. Among various materials Co has been reported as one of the most efficient dopant to ZnO. Even small amount of Co can greatly impart additional functionalities in ZnO material. It is also expected that Co_3O_4 doping on ZnO may enhance the antibacterial activity of the synthesized material.

2. Experimentation

2.1. Materials and methods

ZnO about 99.9999 % pure and pure Co_3O_4 were used [16] and taken after weighing with the help of digital balance. Both ZnO and pure Co_3O_4 were calcinated at 400 ^{0}C for 4 hours in the muffle furnace separately. After calcination process ZnO and Co_3O_4 were grinded separately for 30-40 minutes until both got fine powder with the help of stone spice grinder. Now both the materials were mixed and grinded according to molar concentration of 2% 4% 6% 8% and 10% of dopant Co_3O_4 in the host ZnO with 98% 96% 94% 92% and 90% respectively.

2.2. Pallet formation & sintering

After doping, pallets of 2% 4% 6% 8% and 10% of dopant Co_3O_4 [17] in the host ZnO were formed with the help of hydraulic press by applying 9000 psi pressure. Each pallet weight was about 0.40g and the pallets width is about 2 mm, while compaction time was 50 seconds per pallet. Now pallets were sintered in the furnace at 650^{o}C for 7 h.

3. Results and discussion

3.1. FTIR analysis

FTIR spectroscopy is used to evaluate the bonding characteristics of ZnO. The majority of FTIR spectra peaks fall below 800 cm^{-1}. The stretching and twisting vibrations of the Zn-O bonds are what cause the high intensity peaks at 438, 472, 499, and 519 cm^{-1} [18-19].

Because of the configuration's high degree of symmetry, ZnO peaks are much simpler. Stretching vibrations of ZnO are represented by peaks smaller than 750 cm^{-1}. In Fig: 3.1 (b, c, d, e, f) an absorption around 515cm^{-1}to 700cm^{-1}can be seen which might be due to Co-O stretching frequency [20-21]. The presence of this peak is a good evidence for the synthesis of doped material. This particular peak is missing in Fig: 3.1 (a). The peak at 1437 cm^{-1} relate to the Co adsorption on ZnO surface. Weak absorption band at 1767 cm^{-1} stands for carbonate. A small peak at 1634 cm^{-1}may be due to asymmetric stretch of the zinc carboxylate. These peaks of curves pattern according to transmittance [%] are very satisfying. In these results some impurities near the surface of ZnO are also identified. It can be observed that main peaks at 3400-3600 cm^{-1} are missing [22].

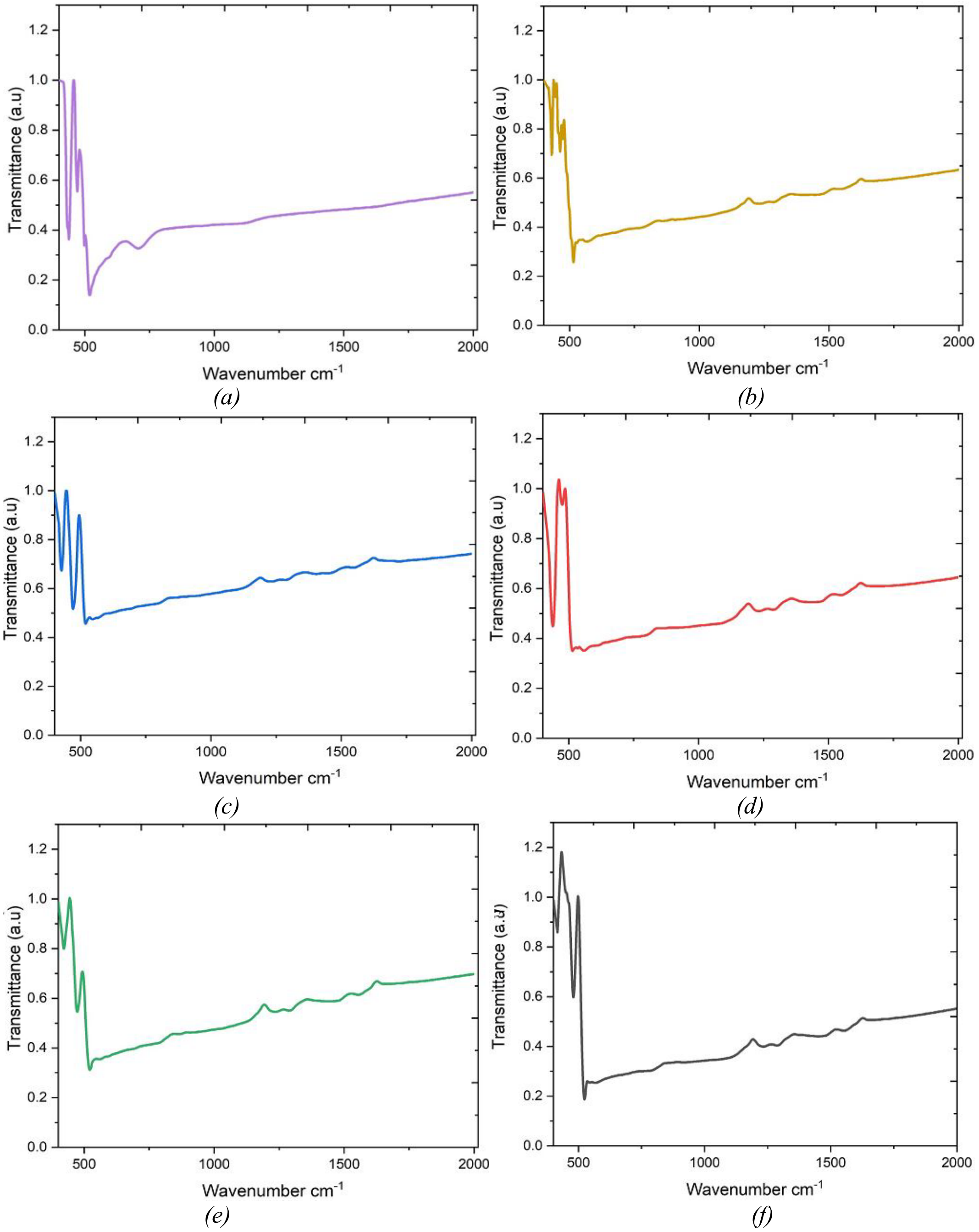

Fig: 3.1 FTIR Spectra of (a) pure ZnO and (b) 2% Cobalt oxide 98% doped ZnO (c) 4% Cobalt oxide 96% doped ZnO (d) 6% Cobalt oxide 94% doped ZnO (e) 8% Cobalt oxide 92% doped ZnO (f) 10% Cobalt oxide 90% doped ZnO.

3.2. Powder X-ray diffraction analysis

To analyze crystal samples accurately and learn more about the structure of crystalline materials, X-Ray Diffraction is used. Zinc oxide crystals with sharp peaks appear in the Fig: 3.2 (a) and the dopant samples for different concentration of Co_3O_4 dopant 2% 4% 6% 8% and 10% are shown in Fig: 3.2 (b), (c), (d), (e), and (f). X-Ray Diffraction patterns confirm the development of the hexagonal wurtzite structure and the purity of phase. XRD peaks in Fig: 3.2 (b-f) are indexed to (102), (110), (103), (202), (112), (201), (004) and (202) reflection planes at 2ϴ values 32.07º, 35.64º, 38.06º, 47.06º, 56.98º, 62.78º, 66.47º, 68.65º,69.06º,72.76ºand 78.65º respectively.

Peaks identified by XRD examination coincide with those on JCPDS Card #36-1451, indicating the purity of the hexagonal wurtzite structure.

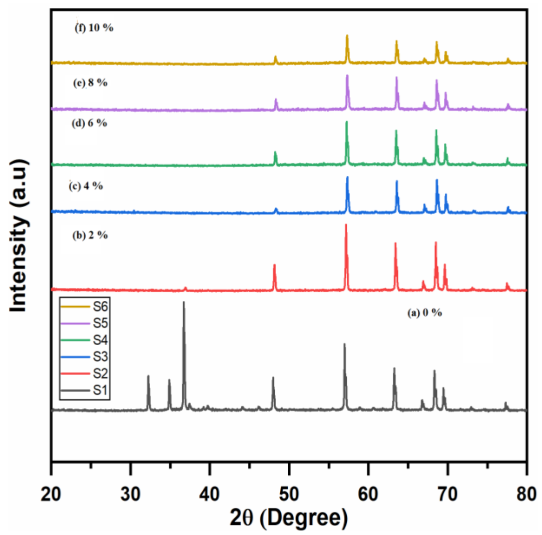

Fig: 3. 2 XRD Pattern for Pure and Doped Samples.

No additional peaks detected in Fig: 3.2, which shows that the bulk of Co ions either occur as contamination phases in the cobalt doped specimen, indicating the existence of cobalt in ZnO material, or are incorporated in the wurtzite-phase crystal lattice which signifies presence of Cobalt in ZnO material. Fig: 3.2 (b-f) demonstrate that the hexagonal wurtzite phase's crystalline behavior is enhanced by the presence of cobalt in ZnO nanoparticles. As dopant element Cobalt was increased from 0 % to 10%, peaks were shifted lower angle to higher angles due to decrease in ionic radii.

Using Scherrer's equation, the average crystallite size (D) is determined from XRD examination for different diffraction angles. Crystallite size (D) is measured in nanometer. X-ray wavelength (λ) possesses a typical value of about 1.54Å. The shape factor (K) which typically have a value between (0.9-0.99) varies according to the crystallites specific shapes.

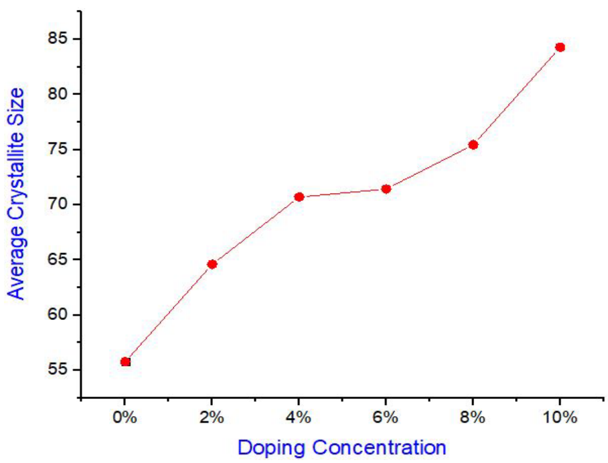

Fig: 3. 3 Graph between Average Crystallite size and Doping Concentration.

The average crystallite size varies between 55 nm and 84 nm which show increase in crystallite size from 2% to 10% doping of Co_3O_4.

3.3. Mechanical properties

Mechanical properties of Co_3O_4 doped ZnO have been measured by using Vicker Hardness indentation Process. The graph between Vicker Hardness (HV) and doping concentration is shown below. In this, measured values of Vicker hardness (HV) are 80, 49,22, 17,14,and 11 at the doping concentration 0%, 2%, 4%, 6%, 8%, 10%, of Co_3O_4 doped in ZnO respectively.

Table: 1 Doping concentration and Vicker Hardness.

Sr.No	Doping concentration	Vicker Hardness (HV)
1	0%	80
2	2%	49
3	4%	22
4	6%	17
5	8%	14
6	10%	11

This graph shows that the hardness of Co_3O_4 doped ZnO pallets decreases as we go from 0% doping to 10% doping. Pure sample has maximum hardness but by increasing doping level from 2-6 % hardness decreases abruptly due to increase in crystallite size.

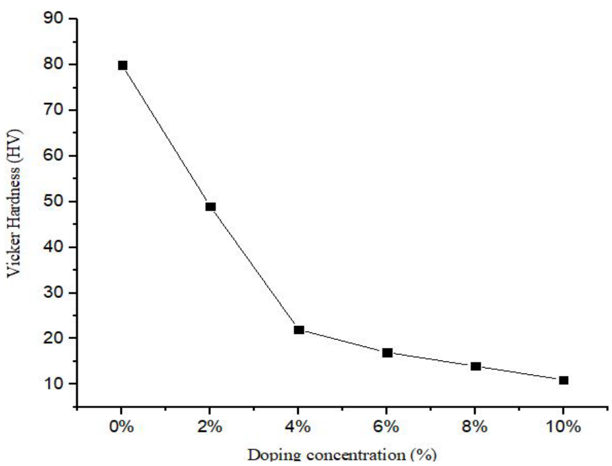

Fig: 3.4 Doping Concentration Graph VS HV.

The Vickers hard test is mostly used for making suitable of welds and metals. The Vickers hardness test, 136^o pyramidal diamond indenter is used that forms a square indent. The two axes of the diamond shaped indentation measured in millimeters are averaged and the hardness is determined, based on a calibration for different kilogram loads. Above graph represents the decrease in Vickers hardness by increasing the doping contents. It means that the addition of doping material can substantially suppress microcracking of ZnO and consequently Vickers hardness is decreased. This decrease is probably due to the weakness of the coupling between the grains and elimination of pores, which may occur during heat treatments. Since ZnO is a n-type semiconductor and Co_3O_4 is a p-type semiconductor so ZnO doped with Co_3O_4 material can be used in synthesis of gas sensing materials.

3.4. Antibacterial activity of Co_3O_4 doped ZnO

It is reported that various metal and metal oxide nanoparticles used as antimicrobial agents [23-25]. The agar well diffusion assay method was used to assess the antimicrobial activity of pure ZnO nanoparticles and Co_3O_4 doped Zno materials against two gram positive bacterial strains, namely *S. Aureus* and *B. subtilis*, and three gram-negative strains, including *E. Coli* and *S. typhi* method [26]. Results are presented in Table 2.

Table: 2 Zone of inhibition of pure ZnO and doped ZnO NPs.

Samples	Diameter of Inhibition zone (mm)			
	Gram Positive		Gram Negative	
	S. aureus	*B. subtilis*	*S. typhi*	*E. coli*
Pure ZnO	10 ± 0.38	11 ± 1.45	12 ± 1.10	14 ± 2.25
2 % Co_3O_4 doping	10 ± 0.70	12 ± 0.25	13 ± 0.41	15 ± 0.51
4 % Co_3O_4 doping	14 ± 1.10	13 ± 1.05	15 ± 0.15	17 ± 0.28
6 % Co_3O_4 doping	16 ± 0.49	16 ± 1.31	17 ± 1.06	19 ± 1.25
8 % Co_3O_4 doping	17 ± 2.10	16 ± 1.04	19 ± 0.41	20 ± 0.25
10 % Co_3O_4 doping	17 ± 2.50	17 ± 1.41	20 ± 0.80	22 ± 1.31

Pure ZnO and doped ZnO showed good antibacterial activity against selected bacterial strains. All synthesized materials found to be effective against bacterial strains but there is a continuous increase in zone of inhibition by increasing the dopant concentration from 2-10 %. It is obvious that Co_3O_4 doping increases the effectiveness of ZnO NPs against various pathogens. Zone of inhibition of synthesized materials against different pathogens are shown graphically in Fig: 3.5.

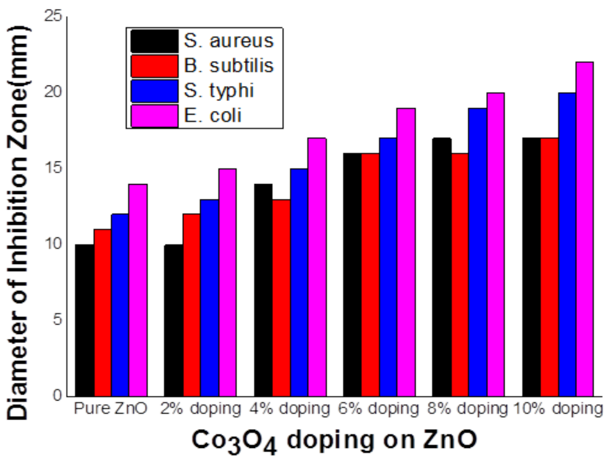

Fig: 3. 5 Zone of inhibition of pure ZnO and doped ZnO NPs.

Table: 3 MIC values of various samples against different bacterial strains.

Samples	MIC values of various bacterial strains (µg/ml)			
	Gram Positive		Gram Negative	
	S. aureus	*B. subtilis*	*S. typhi*	*E. coli*
Pure ZnO	30	35	30	25
2 % Co_3O_4 doping	28	35	28	20
4 % Co_3O_4 doping	25	30	25	15
6 % Co_3O_4 doping	20	25	20	15
8 % Co_3O_4 doping	15	20	15	12
10 % Co_3O_4 doping	15	20	12	10

The MIC values of pure ZnO against different pathogens were found in the range of 25-35 µg but by adding dopant i.e Co_3O_4, MIC values decreases regularly from 2-10 % Co_3O_4 doping. MIC values are inversely proportional to the effectiveness of synthesized material against bacterial strains so 10 % Co_3O_4 doping was found to be most effective i.e 10-20 µg.

It can be concluded that Co_3O_4 doping can inhibit bacterial cell growth and multiplication. This inhibition in growth may be due to the penetration through cell membrane which finally leads to bacterial cell lysis.

4. Conclusion

Pallets formed by doping Co_3O_4 at concentration 0%, 2%, 4%, 6%, 8%, 10%, in ZnO by powder metallurgy method found to be non-homogeneous and non-uniform. XRD results showed that Co ions incorporated on ZnO ions having hexagonal wurtzite structure. It can be seen that crystallite size increases with increasing dopant. The hardness of Co_3O_4 doped ZnO pallets decreases from 0-10 % doping but antibacterial activity increases by adding dopant concentration from 0-10 %.

References

[1] Bagnall D M, Chen Y F, Shen M Y, Zhu Z, Goto T and Yao T, J. Cryst. Growth, 184 605-9 (1998); https://doi.org/10.1016/S0022-0248(98)80127-9

[2] Dhamodharan P, Gobi R, Shanmugam N, Kannadasan N, Poonguzhali R and Ramya S, Spectrochim Acta A Mol Biomol Spectrosc 131 125-31 (2014); https://doi.org/10.1016/j.saa.2014.04.083

[3] Djurišić A B, Ng A M C and Chen X Y, Prog. Quantum Electron. 34 191-259 (2010); https://doi.org/10.1016/j.pquantelec.2010.04.001

[4] C. Kim, H. Hlaing, I. Kymissis, Organic Electronics 36 45-49 (2016); https://doi.org/10.1016/j.orgel.2016.05.031

[5] X. Liu, G. Qiu and X. Li, Nanothechnology, Vol. 16 3035-3040 (2005); https://doi.org/10.1088/0957-4484/16/12/051

[6] W. W. Wang, Y. J. Zhu, Material Research Bulletin, Vol. 40 1929-1935 (2005); https://doi.org/10.1016/j.materresbull.2005.06.004

[7] T. Li, S. Yang, L. Huang, B. Gu, Y. Du, Chinese Phys. Lett., Vol. 21 966-969 (2004); https://doi.org/10.1088/0256-307X/21/5/057

[8] T. Li, S. Yang, L. Huang, B. Gu, Y. Du, Nanotechnology, Vol. 15 1479-1482 (2004); https://doi.org/10.1088/0957-4484/15/11/018

[9] Y. Jiang, Y. Wu, B. Xie, Y. Xie, Y. Qian, "Materials Chemistry and Physics", Vol. 74 234-237 (2002); https://doi.org/10.1016/S0254-0584(01)00463-1

[10] N. R. E. Radwan, M. S. El-Shall, H. M. A. Hassan, Applied Catalysis A: General Vol. 331 8-18 (2007); https://doi.org/10.1016/j.apcata.2007.07.005

[11] N. N. Greenwood, A. Earnshaw, "Chemistry of the elements." 4th ed., Pergamon Press, Oxford (1984)

[11] Pan, F., et al., Materials Science and Engineering: R: Reports 62.1: 1-35 (2008); https://doi.org/10.1016/j.mser.2008.04.002

[12] He, Rongliang, Rosalie K. Hocking, and Takuya Tsuzuki, Materials Chemistry and Physics 132.2-3 1035-1040 (2012); https://doi.org/10.1016/j.matchemphys.2011.12.061

[13] He, Rongliang, et al., Journal of nanoparticle research 15.11 2030 (2013); https://doi.org/10.1007/s11051-013-2030-6

[14] E. Asikuzun, Ceramics International, 41, 6326-6334 (2015); https://doi.org/10.1016/j.ceramint.2015.01.061

[15] Chao Wang, Lian-Long Liu, Ai-Ting Zhang, Peng Xie, Jian-Jun Lu, Xiao-Ting Zou, African Journal of Biotechnology vol. 11(44), pp. 10248-10254, 2012; https://doi.org/10.5897/AJB11.3703

[16] Thangeeswari, T., George, A. T., & Kumar, A. A., Indian Journal of Science and Technology,

9 (1).9 (2016); https://doi.org/10.17485/ijst/2016/v9i1/85776

[17] National Research Council, Analysis of engineering design studies for demilitarization of assembled chemical weapons at Blue Grass Army Depot, National Academies Press. (2002)

[18] S. Zandi et al., Physica B: Condensed Matter 406 (17), 3215 (2011); https://doi.org/10.1016/j.physb.2011.05.026

[19] S. Illy-Cherrey et al., Materials Science and Engineering: A 338 (1) 70 (2002); https://doi.org/10.1016/S0921-5093(02)00057-6

[20] M. Lenglet, J. Lopitaux, L. Terrier, P. Chartier, J.F. Koenig, E. Nkeng, and G. Poillerat, J. Phys. IV 03, C9 (1993); https://doi.org/10.1051/jp4:1993951

[21] C.-W. Tang, C.-B. Wang, and S.-H. Chien, Thermochim. Acta 473, 68 (2008); https://doi.org/10.1016/j.tca.2008.04.015

[22] Vanaja, A., & Rao, K. S., Advances in Nanoparticles, 5(1), 83-89 (2016); https://doi.org/10.4236/anp.2016.51010

[23] Alt, V.; Bechert, T.; Steinrcke, P.; Wagener, M.; Seidel, P.; Dingeldein, E.; Domann, U.;Schnettler, R., Biomater. 2004, 25, 4383-4391; https://doi.org/10.1016/j.biomaterials.2003.10.078

[24] Furno, F.; Morley, K.S.; Wong, B.; Sharp, B.L.; Arnold, P.L.; Howdle, S.M.; Bayston, R.; Brown, P.D.; Winship, P.D.; Reid, H., J. Antimicrob. Chemother. 2004, 54, 1019-1024; https://doi.org/10.1093/jac/dkh478

[25] Jeong, S.H.; Yeo, S.Y.; Yi, S.C., J. Mater. Sci. 2005, 40, 5407-5411; https://doi.org/10.1007/s10853-005-4339-8

[26] Perez, C.; Paul, M.; Bazerque, P. Antibiotic assay by agar well diffusion method, Acta Biol.Med. Exp. 1990, 15, 113-115.